Anisotropy of the resistivity and charge-carrier sign in nanolaminated Ti_2AlC: Experiment and *ab initio* calculations

Vincent Mauchamp,[1,*] Wenbo Yu,[1] Loïk Gence,[2] Luc Piraux,[2] Thierry Cabioc'h,[1] Véronique Gauthier,[1] Per Eklund,[3] and Sylvain Dubois[1]

[1]*Institut Pprime, UPR 3346 CNRS - Université de Poitiers - ISAE-ENSMA, SP2MI Téléport 2, BP 30179, 86962 Futuroscope-Chasseneuil Cedex, France*

[2]*Institute of Condensed Matter and Nanosciences, Université Catholique de Louvain, B-1348 Louvain la Neuve, Belgium*

[3]*Thin Film Physics Division, Linköping University, IFM, 581 83 Linköping, Sweden*

(Received 14 November 2012; revised manuscript received 21 March 2013; published 5 June 2013)

The anisotropy of Ti_2AlC transport properties is investigated focusing on the Hall effect and resistivity vs temperature measurements performed on a highly (000l)-oriented thin film and a bulk polycrystalline sample. Experimental data are interpreted on the basis of density functional theory calculations including transport coefficients obtained with the Boltzmann semiclassical transport equation in the isotropic relaxation time approximation. It is shown that the Hall constant is independent of the temperature and that the charge-carrier sign depends on the investigated crystallographic orientation. Charge carriers exhibit a holelike character along the basal plane of the Ti_2AlC, whereas the bulk sample Hall constant is negative. The resistivity anisotropy is also evidenced: using an effective medium approach, the room temperature basal plane resistivity is shown to be more than one order of magnitude lower than that along the c axis. This very important anisotropy is shown to result from the anisotropy of the Fermi surface increased by electron-phonon interactions. These interactions are much more important along the c axis than within the basal plane, a situation opposite to that observed in literature for Ti_2GeC where resistivity was reported to be isotropic.

DOI: 10.1103/PhysRevB.87.235105 PACS number(s): 72.15.−v, 72.80.Ga, 71.18.+y

I. INTRODUCTION

In the search for on-purpose designed materials, the ternary carbides and nitrides with general formula $M_{n+1}AX_n$ ($n = 1$, 2, or 3), M being an early transition metal, A an A-group element (from IIIA to VIA), and X being either C or N, are promising.[1,2] These compounds, named MAX phases from their chemical formula, crystallize in the hexagonal $P6_3/mmc$ space group and can be described as the stacking of M_6X octahedra layers interleaved with pure A element layers. These structures exhibit large c/a ratios, typically 3, 6, and 8 for $n = 1$, 2, and 3, which leads to a very anisotropic unit cell [see the unit cell of Ti_2AlC, which corresponds to $n = 1$, sketched in Fig. 1(a)]. Due to this nanolaminated structure, they combine the best properties of metals and ceramics demonstrating, for instance, high sustainability in extreme environment (high temperature, corrosive, oxidizing) and very good electronic properties.[3–6] This unique combination of properties opens a way to diverse potential applications. Of special interest are the titanium-based compounds, intensively investigated for high temperature ohmic contacts on wide gap semiconductors.[7–10]

MAX phase electronic properties and especially the anisotropy resulting from the nanolaminated structure is not yet fully understood. Although intensively studied, it remains a complex issue since the majority of transport experiments were performed on polycrystalline samples, thereby averaging the basal plane and c-axis transport properties.[6,11–13] To circumvent this point, several alternative approaches have been investigated such as the probe of single grains plasmon excitations anisotropy using electron energy-loss spectroscopy (EELS),[14–17] the comparison between data obtained on (000l) oriented thin films and bulk polycrystalline samples,[18] or the comparison between thin films with different grain populations.[19] In the two latter cases, the conductivity anisotropy is evidenced since the (000l) thin film room temperature (RT) resistivities and electron-phonon interactions are different from either the data recorded on the polycrystalline sample or on the thin film exhibiting a different grain population. Moreover, comparison between these results also evidence the importance of the chemical composition of the MAX phase since Scabarozi *et al.* report a basal plane RT resistivity of 0.24 $\mu\Omega$ m in Ti_2GeC, whereas the Cr_2GeC basal plane RT resistivity reported by Eklund *et al.* is twice as large: 0.51 $\mu\Omega$ m.

In all cases, the transport properties were qualitatively understood using phenomenological two band models or, at best, by comparing with band structure calculations. However, the calculations of transport properties is sometimes mandatory for a quantitative understanding of these compounds electronic properties. This was demonstrated by Chaput *et al.* who showed that the negligible Seebeck coefficient of a polycrystalline Ti_3SiC_2 sample could be understood from the compensation of electronlike states along the c axis by holelike states within the basal plane orientation at the Fermi level.[5,20,21] An accurate description of both the electronic structure and the transport properties is all the more desirable that MAX phases exhibit complex Fermi surfaces with generally more than two bands [see Fig. 1(b) for Ti_2AlC],[22] and that the chemical bonding in these materials is based on complex charge transfers involving metallic, ionic, and covalent bonds.[23]

The aim of this paper is to understand the anisotropy of Ti_2AlC transport properties by characterizing both charge carriers and the anisotropy of the resistivity. Temperature dependent Hall coefficients and resistivity measurements were performed on two samples: an epitaxial (000l) Ti_2AlC thin film and a bulk polycrystalline sample. Experimental results are understood on the basis of band structure density functional theory (DFT) calculations which are used to compute the

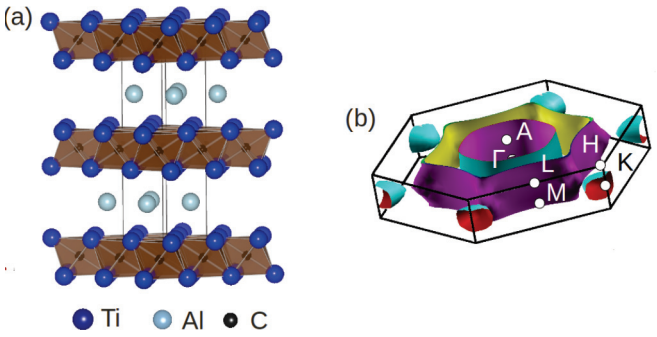

FIG. 1. (Color online) (a) Unit cell and (b) Fermi surface of Ti_2AlC. For details about the calculation, see Sec. III.

transport properties in a semiclassical framework. The paper is organized as follows. First, the experimental details concerning sample elaboration and transport properties measurements are described. In the second part, the calculation details are given. Then, experimental results are given and compared to calculations and the anisotropy of the transport properties is discussed.

II. EXPERIMENT AND MATERIAL PROCESSING

The epitaxial (000l) Ti_2AlC MAX-phase thin films were synthesized under ultrahigh vacuum (UHV) conditions by unbalanced (type II) dc magnetron sputtering using high purity elemental targets.[24,25] The deposition process was carried out at a constant pressure of 0.5 Pa in high purity Ar (99.9999%) discharges. Thin film was grown at 900 °C on Al_2O_3 (0001) substrates preseeded with a thin epitaxial TiC layer.

Powders of Ti (<45 μm, 99.5% purity), Al (<45 μm, 99.5% purity), and TiC (2 μm, 99.5% purity), with the nominal composition 1.15Ti:1.05Al:0.85TiC, were used to synthesize Ti_2AlC bulk sample. Powders were milled for 4 h in a Turbula mixer (WAB). The reactant mixtures were then cold compacted into cylindrical steel dies using an uniaxial pressure of 100 MPa. Afterwards, the green samples were encapsulated into Pyrex containers under high vacuum for reactive sintering in the hot isostatic press (HIP) machine. The green samples were subjected to the following temperature and pressure cycles.

(i) The samples were heated up to 1400 °C (heating rate = 35 °C/min), while the Ar pressure was increased up to 80 MPa (pressure rate = 1.2 MPa min^{-1}).

(ii) Once the processing temperature and pressure were reached, the samples were held for 4 h.

(iii) Cooling the furnace to room temperature and decreasing the pressure to atmospheric pressure proceeds in 90 min.

After HIPing, samples were machined to remove the encapsulating glass container and sliced using a diamond wheel. Samples were thus grinded, down to about 30 μm, using silicon carbide paper and then polished with a diamond suspension. Finally, a chemomechanical polishing has been performed using a neutral suspension of alumina particles. Such a chemomechanical polishing allows for producing a very flat surface.

Measurements of the resistivity were carried out on both samples, in the temperature range 15–295 K, in a Van der Pauw geometry. The (000l)-oriented film thickness is 140 nm, whereas the polycrystalline bulk sample is 26.5 μm thick. Wavelength dispersive x-ray spectroscopy (WDS) was used to determine the carbon stoichiometry in the two samples. Experiments were performed at ICMCB (Bordeaux, France) with pyrolytic carbon as a standard: the carbon stoichiometries were found to be almost identical, 0.82 and 0.85 for the thin film and bulk sample, respectively, with a standard deviation of 0.05. The carbon stoichiometry of the bulk sample was confirmed by WDS measurements performed at Pprime Institute (Poitiers, France) with SiC as a standard [pure SiC (>99.9%) provided by Micro-Analysis Consultants Ltd. (MAC) (number: S59-04-14173; part number: S4-5030-M)]: the carbon content was found to be 0.84.

III. CALCULATION DETAILS

Band structure calculations were performed with the WIEN2K code, an all electron full potential approach based on a linearized augmented plane wave (LAPW) method.[26] Augmented plane waves (APW) combined with local orbitals (APW + lo) were used with a converged basis set obtained for a RK_{max} value of 7.5.[27] Calculations were performed considering the Perdew-Burke-Ernzerhof generalized gradient approximation,[28] 800 k points were used in the full Brillouin zone for the self-consistent field determination of the potentials. Optimized unit cell parameters were considered: $a = 3.04$ Å, $c = 13.60$ Å, and $z_{Ti} = 0.0845$, z_{Ti} being the only free parameter in the space group. These values are in very good agreement, to within less than 1%, with the experimental ones deduced from x-ray diffraction and extended absorption fine structures refinements.[23]

The band structure calculations were used to compute the Fermi surface using the Xcrysden software,[29] and as an input for the Hall and conductivity tensors calculations. These transport coefficients were computed in the framework of the semiclassical Boltzmann theory, considering the relaxation time approximation, in a rigid band approach using the BOLTZTRAP code.[30] Transport coefficient are computed from the transport distribution:

$$\sigma_{\alpha,\beta}(\varepsilon) = \frac{1}{N}\sum_{i,\mathbf{k}} \sigma_{\alpha,\beta}(i,\mathbf{k})\frac{\delta(\varepsilon - \varepsilon_{i,\mathbf{k}})}{d\varepsilon}, \quad (1)$$

which is expressed in terms of the **k**-dependent transport tensor, given by

$$\sigma_{\alpha,\beta}(i,\mathbf{k}) = e^2\tau_{i,\mathbf{k}}v_\alpha(i,\mathbf{k})v_\beta(i,\mathbf{k}), \quad (2)$$

where $\tau_{i,\mathbf{k}}$ is the relaxation time and $v_{\alpha,\beta}(i,\mathbf{k})$ the group velocity. The transport coefficients are then calculated as a function of the temperature and the chemical potential by integrating the transport distribution (see Ref. 30 for details). Since the details of the scattering mechanisms are unknown, so is $\tau_{i,\mathbf{k}}$. In the present approach, it is assumed to be constant and isotropic so that the Hall coefficient becomes independent of τ and can be compared directly to the experiment. Concerning the conductivity, we only have access to the Fermi surface dependent quantity: $\zeta_{ii} = \sigma_{ii}/\tau_{ii}$. Note that, although ζ_{ii} cannot be compared directly to the experimental conductivity, for isotropic relaxation time the ratio ζ_{xx}/ζ_{zz} is independent of τ and can be compared to the ratio of the experimental

conductivities. The isotropic relaxation time approximation was successfully used for the calculation of the anisotropy of 312 MAX phases thermopower. Calculations were performed using a fine k mesh of 200 000 k points in the full Brillouin zone ensuring a convergence of the Hall coefficient to within 10%.

IV. RESULTS AND DISCUSSION

A. Hall constants

The Hall resistivity recorded as a function of the magnetic field at 25 K, 150 K, and RT on the Ti_2AlC (000l) thin film and at RT on the bulk sample is sketched in Fig. 2. Only RT measurements could be performed on the bulk sample since the Hall voltage was very weak [typically a hundred times lower than that for the (000l) film], so that temperature variations led to important fluctuations. In all cases, the variation of the Hall resistivity is linear, whereas its sign depends on the relative orientation of the current and the Ti_2AlC crystal. For the current flowing in the Ti_2AlC basal plane, the Hall resistivity is definitely positive, whereas it is negative for a current flowing in the Ti_2AlC bulk sample. The Hall constants extracted from these curves are -3.4×10^{-10} and $+2.2 \times 10^{-10}$ m^3C^{-1} for the bulk sample and thin film, respectively. The experimental bulk value is in good agreement with the one measured by Scabarozi *et al.* on a similar sample, -2.8×10^{-10} m^3C^{-1}, with very weak variations with the temperature.[13]

Phenomenologically, the weak temperature dependence of the basal plane Hall constant, as measured on the film, justifies the interpretation of basal plane MAX phase transport properties in terms of a single band model (holelike states in Ti_2AlC). On the other hand, the opposite sign of the trace of the Hall tensor compared to the one of the basal plane Hall constant justifies the interpretation of MAX phase transport properties in terms of a two band model, with electronlike and holelike states, respectively, along the c axis and in the basal plane. This model is consistent with the holelike and electronlike behaviors observed respectively in the basal plane and along the c axis of M_3AX_2 phases.[22] It is thus possible to extract, from the basal plane Hall constant

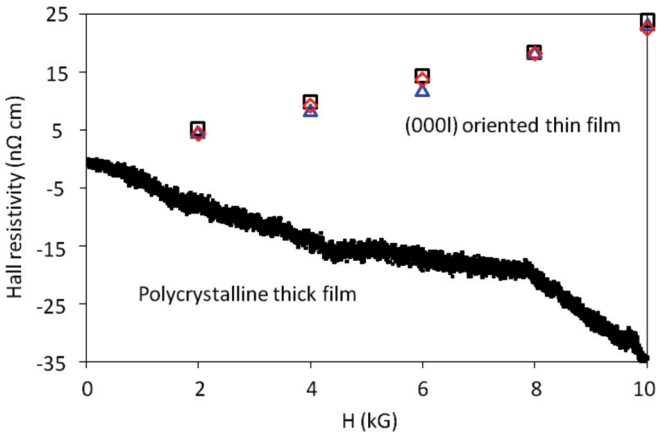

FIG. 2. (Color online) Hall resistivity recorded as a function of the magnetic field at 25 K (black squares), 150 K (blue triangles), and RT (red diamonds) on the (000l) Ti_2AlC thin film and at RT on the bulk sample.

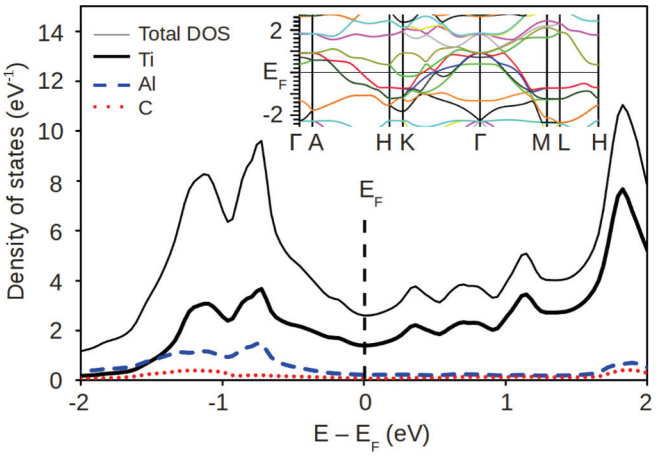

FIG. 3. (Color online) Ti_2AlC site projected density of states and the corresponding band structure calculated along the high symmetry points of the first Brillouin zone.

measurement, the charge carriers density. In this single band model, holelike carriers density (p) can be estimated from the relation $R_H = 1/pe$ which leads to $2.8 \times 10^{+28}$ m^{-3}. This value is in quite good agreement with results deduced from heat capacity measurements ($\approx 3.8 \times 10^{28}$ m^{-3}).[31,32] The deduced charge-carrier mobility in the basal plane is thus, at RT, 1.1×10^{-3} $m^2V^{-1}s^{-1}$ [estimated from the ideal resistivity at RT; see Fig. 4(b)].

By comparing these results with the ones obtained by Scabarozi *et al.*, who assume a two band model,[13] one can notice that our values are one order of magnitude higher for the holelike concentration and five times lower for the mobility. Such a discrepancy can be ascribed to their hypothesis of equal electronlike and holelike mobilities. This equality is questionable given the important band dispersion anisotropy evidenced in the band structure sketched in Fig. 3: the bands show an important dispersion along reciprocal lattice directions corresponding to the basal plane ($\Gamma \rightarrow M$ or $\Gamma \rightarrow K$), whereas their dispersion is very weak along directions corresponding to the c axis ($\Gamma \rightarrow A$, $H \rightarrow K$, or $L \rightarrow M$). This results in an important anisotropy in the band velocities. Moreover, as will be seen in the next paragraph, the electron-phonon interaction is also very anisotropic.

The experimental Hall constants are compared to the *ab initio* calculations in Table I. Assuming that the bulk sample displays randomly oriented grains, the R_H value is compared to the trace of the Hall tensor whereas the thin film data are compared to the $R_{H,xyz}$ component determined from the geometry of the experiment. The calculated values are in qualitative agreement with the experiments. The R_H signs are confirmed for both the (000l) thin film and the bulk sample, confirming that the transport properties along the MAX phase basal plane are governed by holelike electron states. However, the relative error between the experimental data and the calculations in the thin film is much higher than that for the bulk sample: 50% and 10%, respectively. The error for the bulk sample is very similar to that resulting from the k point sampling, which gives strong support to the calculation. In contrast, the error between the theoretical value of $R_{H,xyz}$ and

TABLE I. Ti_2AlC temperature dependent Hall constants (R_H), room temperature ideal resistivities (ρ), and slopes of the $\rho(T)$ curves measured on the bulk sample and the (000l) oriented thin film. The Hall constants obtained from the *ab initio* calculations are also given for comparison. The resistivity along the c axis deduced from the effective medium (E.M.) approach considering elongated spheroids with an aspect ratio of 2.5 is also given (see Sec. IV B for details).

Sample	$R_{H,\text{expt}}$ (m^3C^{-1})	$R_{H,\text{theor}}$ (m^3C^{-1})	ρ ($\mu\Omega\,cm$)	$\partial\rho/\partial T$ ($\mu\Omega\,cm\,K^{-1}$)
Bulk sample	-3.4×10^{-10} at RT	-3.7×10^{-10}	37	0.18
(000l)-oriented sample	$+2.2\times10^{-10}$ at 25 K, 150 K, and RT	1.0×10^{-10}	20	0.10
c axis (deduced from E.M.)			347	1.75

the experimental one is almost 50%. One possible explanation is the failure of the isotropic relaxation time approximation used for the transport properties calculations. The good results obtained for the bulk sample could then be due to cancellation of errors between the different components of the Hall tensor when computing the trace. This is in agreement with recently published results on the Seebeck coefficient of Ti_3SiC_2,[21] where it is shown that the in-plane component obtained with similar calculations is 25% lower than the experimental value at room temperature, whereas the trace of the Seebeck coefficient gave very good results compared to experimental data obtained on a polycrystalline sample.[20]

The validity of the isotropic relaxation time approximation is however not directly comparable between Hall constants and Seebeck coefficient. Indeed, the application of a magnetic field in the former case modifies the symmetry constraints that the relaxation time must fulfill. Chaput *et al.* investigated this problem in elemental zinc and showed that if the relaxation time is assumed to be constant for the calculation of the Hall tensor, then it must also be isotropic.[33] Our results suggest that the relaxation time is most probably anisotropic so that a constant relaxation time approximation is not satisfactory for the description of the the Hall tensor. In particular, although dominated by the titanium d bands, the complex electronic structure at the Fermi level of Ti_2AlC also involves aluminum and carbon character (see the site projected density of states in Fig. 3), so that one would expect a **k** dependent relaxation time (i.e., dependent of the Bloch state character). Such an approach involving different relaxation times for the different angular momenta of the wave functions at the Fermi level was demonstrated to greatly improve the calculation of the aluminum Hall constant when compared to the experiment.[34]

B. Resistivity

Figure 4(a) shows the Ti_2AlC resistivity variations as a function of the temperature. The RT and residual resistivities are 36 $\mu\Omega\,cm$ and 16 $\mu\Omega\,cm$, respectively, for the (000l)-oriented thin film and 65 $\mu\Omega\,cm$ and 27 $\mu\Omega\,cm$ for the bulk sample. The RT and residual resistivities of the (000l)-oriented film are in the same range as the ones determined on bulk samples by Hettinger *et al.* and very close to that reported for a thin film by Magnuson *et al.* (40 $\mu\Omega\,cm$).[11,35] The values obtained on the bulk sample are larger. This implies that defects limit the mean free path at low temperature. By using Mathiessen's rule, one can extract the ideal resistivity ρ_i which is given by

$$\rho_i(T) = \rho(T) - \rho_0, \tag{3}$$

ρ_0 being the residual resistivity. The ideal resistivity, depicted in Fig. 4(b), only depends on the charge-carrier scattering mechanism (i.e., it does not depend on defect and impurity densities). At RT, the ideal resistivities are 20 and 37 $\mu\Omega\,cm$ for the (000l) film and the bulk sample, respectively (the bulk sample resistivity is in excellent agreement with the one reported by Scabarozi *et al.*[13]). These values are summarized in Table I. This evidences the resistivity anisotropy of this nanolaminated compound. As usually observed in MAX phases, ρ_i varies linearly with the temperature in the range 150–300 K and one can calculate the slope of the linear variation. The slopes are 0.10 and 0.18 $\mu\Omega\,cm\,K^{-1}$ for the (000l)-oriented thin film and the bulk polycrystalline sample, respectively.

The thin film resistivity is in good agreement with measurements carried out on other Ti_2AlC samples for which $\partial\rho/\partial T$ is in the range 0.067–0.1 $\mu\Omega\,cm\,K^{-1}$. Nevertheless, one can notice that the slope obtained for the bulk sample is higher than previously reported values. Such a behavior can be ascribed to the presence of vacancies and the disorder that they induce in the structure. That vacancies are strong electron scatterers is evidenced in the high residual resistivity that we find, 27 $\mu\Omega\,cm$, compared to that reported by Scabarozi *et al.*, 7 $\mu\Omega\,cm$. Although the details of the scattering mechanism are unknown, equivalent increase of the $\rho(T)$ slope with disorder or vacancies concentration is also observed in metals or semimetals exhibiting the same linear $\rho(T)$ tendency as that observed in MAX phases.[36,37]

Given that the thin film and the bulk sample exhibit very similar compositions, one can extract the c-axis resistivity (ρ_{zz}) from these two curves. As Scabarozzi *et al.* did for Ti_2GeC,[18] we use an effective medium (E.M.) approach

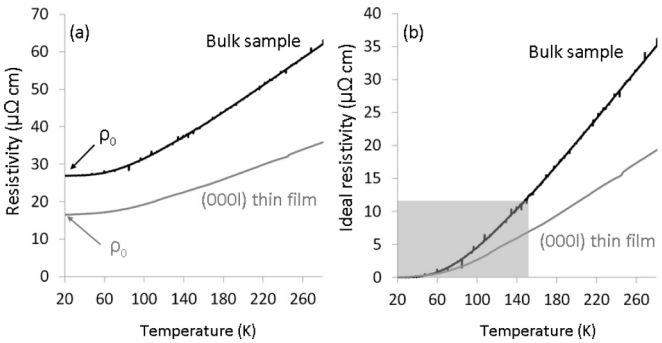

FIG. 4. Resistivity vs temperature: (a) raw data obtained on the (000l) thin film and the bulk polycrystalline sample; (b) corresponding ideal resistivities.

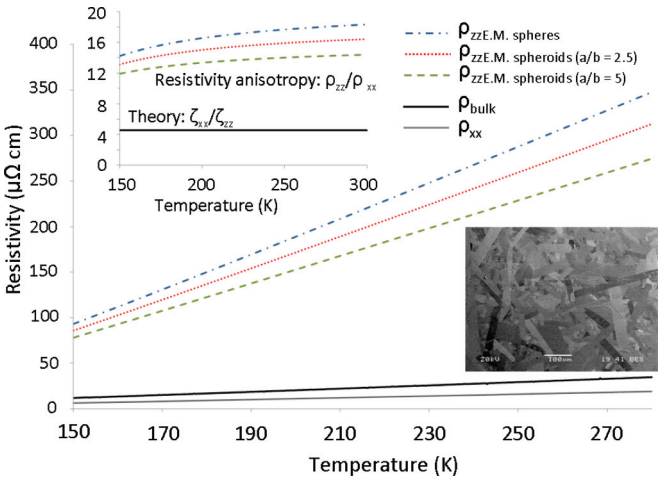

FIG. 5. (Color online) ρ_{zz} obtained from the effective medium approach considering spherical grains (blue dotted-dashed line), spheroids with an aspect ratio $a/b = 2.5$ (red dots), and $a/b = 5$ (green dashed line). For comparison, ρ_{xx} and ρ_{bulk} are also given: gray and black curve, respectively. Inset: resistivity anisotropy, ρ_{zz}/ρ_{xx}, deduced from these curves and compared to the Fermi surface anisotropy obtained from ζ_{xx}/ζ_{zz}. A scanning electron microscopy micrograph is also given to show the grain shape of the bulk sample.

assuming spherical grains:[38]

$$\frac{2(\sigma_b - \sigma_{xx})}{2/3\sigma_b + 1/3\sigma_{xx}} + \frac{(\sigma_b - \sigma_{zz})}{2/3\sigma_b + 1/3\sigma_{zz}} = 0, \tag{4}$$

where σ_b is the bulk conductivity. The corresponding curve is plotted in Fig. 5. Contrary to what is observed for Ti_2GeC, the E.M. approach evidences a very important anisotropy of the resistivity, ρ_{zz} being more than 20 times higher than ρ_{xx}. This value most probably overestimates the anisotropy because of the assumption of spherical grains, which is not realistic considering the scanning electron microscope (SEM) image of the sample (see Fig. 5). In order to investigate the influence of the grains shape, ρ_{zz} has been extracted from an E.M. approach considering elongated spheroid grains with an aspect ratio $a/b = 2.5$ or $a/b = 5$, systems much closer to the true configuration. In such cases, the equation fulfilled by σ_{xx}, σ_{zz}, and σ_b is[38]

$$p\left[\frac{\sigma_{xx} - \sigma_b}{\sigma_b + g_{\parallel}(\sigma_{xx} - \sigma_b)} + \frac{2(\sigma_{xx} - \sigma_b)}{\sigma_b + g_{\perp}(\sigma_{xx} - \sigma_b)}\right] + (1-p)\left[\frac{\sigma_{zz} - \sigma_b}{\sigma_b + g_{\parallel}(\sigma_{zz} - \sigma_b)} + \frac{2(\sigma_{zz} - \sigma_b)}{\sigma_b + g_{\perp}(\sigma_{zz} - \sigma_b)}\right] = 0. \tag{5}$$

In this expression, p is the volume fraction of grains oriented along the basal plane. Supposing that the grain orientation is averaged in the bulk sample, which according to the results obtained on the trace of the Hall constant seems to be a reasonable approximation, we took $p = 2/3$. $g_{\parallel}$ and $g_{\perp}$ are the depolarization factors corresponding to the major axis and the transverse direction of the spheroid. The expressions of these factors can be found in Ref. 39, Sec. 4. For the particular case of spherical grains, one has $g_{\parallel} = g_{\perp} = 1/3$ and Eq. (5) reduces to Eq. (4). The ρ_{zz} deduced from this Eq. (5) for aspect ratios $a/b = 2.5$ and 5 are compared to the E.M. with spherical grains in Fig. 5. Although ρ_{zz} is reduced when considering elongated grains, it is still far more important than the basal plane resistivity with RT resistivities ranging from 347 $\mu\Omega$ cm to 290 $\mu\Omega$ cm depending on the aspect ratio considered in the effective model. Compared to ρ_{xx} the deduced resistivity is more than one order of magnitude larger. The slope of $\rho_{zz}(T)$ is also very important compared to that obtained along the basal plane. The values vary from 1.97 $\mu\Omega\,\text{cm}\,\text{K}^{-1}$ for the model with spherical grains to 1.59 $\mu\Omega\,\text{cm}\,\text{K}^{-1}$ for the spheroids with $a/b = 5$. These values are here again much higher than that obtained on the thin film (0.10 $\mu\Omega\,\text{cm}\,\text{K}^{-1}$).

Although our E.M. approach can only give a crude estimate of the anisotropy, the results obtained are in reasonable agreement compared to the RT optical conductivities obtained from ellipsometry.[40] In these experiments performed in reflexion, the signal retrieved from the polycrystalline sample is the average between the basal plane and c-axis response: $\rho_{\text{bulk}} = \frac{1}{3}(2 * \rho_{xx} + \rho_{zz})$. This is a big difference with transport measurements where the current flow is influenced by the respective resistivity of the different grains and explains why the resistivity deduced from ellipsometry is generally superior to that obtained from four points probe measurements in MAX phases. Taking the ρ_{xx} and ρ_{zz} values deduced from our models, we obtain an average resistivity of 130 $\mu\Omega$ cm taking an aspect ratio $a/b = 2.5$ and 110 $\mu\Omega$ cm taking an aspect ratio $a/b = 5$. These values are in qualitative agreement with the ellipsometry data: 84 $\mu\Omega$ cm. Here, again, the higher value that we obtain can be explained by the disorder induced by the vacancies. This phenomenon has already been observed in niobium carbides, for instance, where the optical conductivity is reduced by almost a factor of 3 for 13% of vacancies on the carbon site when compared to the stoichiometric compound.[41]

In order to get more insight into Ti_2AlC resistivity anisotropy, the ρ_{zz}/ρ_{xx} ratio is plotted as a function of the temperature in the inset of Fig. 5 and compared to the anisotropy of the Fermi surface velocities distribution as deduced from the ratio ζ_{xx}/ζ_{zz}. It appears clearly that ρ_{zz}/ρ_{xx} is large, between 14 and 18, and weakly dependent on the temperature in the 150–300 K temperature range. This anisotropy is a combination of the Fermi surface anisotropy (see Fig. 1) and the scattering mechanisms. From the electronic structure point of view, Ti_2AlC already evidences an important resistivity anisotropy since the ζ_{xx}/ζ_{zz} ratio gives a resistivity almost five times higher along the c axis than within the basal plane. This anisotropy is drastically increased to more than one order of magnitude by the scattering mechanisms which, from the linear dependence of the $\rho(T)$ curves, are most probably dominated by electron-phonon interactions: these results reveal a stronger electron-phonon interaction along the c axis than within the basal plane of the MAX phase as previously observed in Cr_2GeC.[19] They also evidence the important interplay between electronic structure and scattering mechanisms in the MAX phases transport properties. Note that in other materials such as elemental zinc, the electron-phonon interaction tends to compensate the Fermi surface anisotropy so that this material exhibits a very weak resistivity anisotropy.[33] Such a mechanism is a possible explanation for the very different behavior observed between Ti_2GeC and Ti_2AlC: in Ti_2GeC the slope of $\rho(T)$ for the bulk sample is lower than that recorded on (000l) thin films (0.084 $\mu\Omega\,\text{cm}\,\text{K}^{-1}$ and 0.1 $\mu\Omega\,\text{cm}\,\text{K}^{-1}$,

respectively) evidencing weaker electron-phonon interactions along the *c* axis than within the basal plane in this compound.[18] This is totally different from what we observe in Ti_2AlC.

V. SUMMARY AND CONCLUSION

The anisotropy of Ti_2AlC transport properties has been investigated focusing on a (000l) oriented thin film, giving access to the basal plane response of the MAX phase, and a bulk highly pure polycrystalline sample of similar composition. Both temperature dependent Hall effect and resistivity measurements were performed and interpreted thanks to *ab initio* calculations.

Concerning Hall effects measurements, the anisotropy of the Fermi surface resulting from the nanolaminated structure is evidenced through a change of the charge carriers sign with the crystallographic orientation. Given that the Hall constants of both samples are weakly dependent on the temperature, our results justify the interpretation of MAX phases polycrystalline bulk samples transport properties in terms of a two band model, one describing the holelike behavior within the basal plane and one describing the electronlike behavior along the *c* axis of the structure.[11,13] This behavior is moreover consistent with that observed in 312 MAX phases.[20,22] Considering a single band model and a holelike state to account for the basal plane Hall constant, the charge-carrier density is found to be $2.8 \times 10^{+28}$ m^{-3}, a value in good agreement with others deduced from heat capacity measurements.[31,32] The charge-carrier mobility is found to be 1.1×10^{-3} $m^2V^{-1}s^{-1}$, a value five times higher than that reported by other authors.[13] We attribute this difference to the fact that they considered equivalent mobilities for electron and holes in their two band models, whereas a careful analysis of either the Fermi surface or the band structure reveals an important band velocity anisotropy when focusing on reciprocal directions corresponding to the basal plane (holelike states) or the *c* axis (most probably electronlike states).

The calculations qualitatively reproduce the experimental results: the charge-carrier signs are confirmed for both the thin film and the bulk sample. The agreement on the absolute value of the Hall constant is however dependent on the crystallographic orientation. It is in good agreement for the bulk sample but the discrepancy is much more pronounced for the R_{hxyz} component corresponding to the thin film data (the relative error is worse than 50%). This discrepancy is understood in terms of a failure of the isotropic relaxation time approximation used in our calculations, which would be canceled in the calculation of the Hall tensor trace. This explanation is coherent with Ti_3SiC_2 Seebeck coefficient data which were recently published.[21]

The resistivity measurements also clearly evidence a strong anisotropy of Ti_2AlC electronic properties. Comparing the data recorded on the thin film to those obtained on the bulk sample, which are interpreted in terms of an effective medium approach, it is shown that the room temperature resistivity ρ_{zz} is more than one order of magnitude larger than ρ_{xx}. The slopes of the $\rho(T)$ curves confirm such an anisotropy, $\partial\rho_{zz}/\partial T \approx 1.75$ $\mu\Omega\,\mathrm{cm\,K^{-1}}$, whereas $\partial\rho_{xx}/\partial T \approx 0.1$ $\mu\Omega\,\mathrm{cm\,K^{-1}}$. Comparison of the experimental data with the anisotropy of the Fermi surface deduced from the *ab initio* calculations reveals that the observed anisotropy is a cumulated effect of the band structure anisotropy and the electron-phonon interaction. This behavior is significantly different from that evidenced in Ti_2GeC with a similar approach where the resistivity was found to be almost isotropic. These results evidence the crucial role of the chemical composition on the transport properties in the MAX phase family. Since, in Ti_2GeC, the electron-phonon interaction is found to be weaker along the *c* axis than within the basal plane, it can be an explanation for the reduced anisotropy observed in this sample. A similar effect was observed in elemental zinc, for instance.[33]

ACKNOWLEDGMENTS

Jenny Frodelius is acknowledged for providing the Ti_2AlC thin film sample. P.E. acknowledges financial support from the Swedish Research Council (VR) through the Linnaeus LiLi-NFM Strong Research Environment and Project Grant No. 621-2009-5258. Michel Lahaye from ICMCB (Bordeaux) and Dominique Eyidi from Pprime Institute (Poitiers) are acknowledged for performing WDS experiments on the Ti_2AlC samples.

*vincent.mauchamp@univ-poitiers.fr

[1] M. W. Barsoum, Prog. Solid State Chem. **28**, 201 (2000).
[2] P. Eklund, M. Beckers, U. Jansson, H. Högberg, and L. Hultman, Thin Solid Films **518**, 1851 (2010).
[3] K. R. Whittle, M. G. Blackford, R. D. Aughterson, S. Moricca, G. R. Lumpkin, D. P. Riley, and N. J. Zaluzec, Acta Mater. **58**, 4362 (2010).
[4] Z. J. Lin, M. S. Li, J. Y. Wang, and Y. C. Zhou, Acta Mater. **55**, 6182 (2007).
[5] H.-Y. Yoo, M. W. Barsoum, and T. El-Raghy, Nature (London) **407**, 581 (2000).
[6] M. W. Barsoum, H.-I. Yoo, I. K. Polushina, V. Yu. Rud', Yu. V. Rud', and T. El-Raghy, Phys. Rev. B **62**, 10194 (2000).
[7] K. Buchholt, R. Ghandi, M. Domeij, C. M. Zetterling, J. Lu, P. Eklund, L. Hultman, and A. Lloyd Spetz, Appl. Phys. Lett. **98**, 042108 (2011).
[8] Z. Wang, S. Tsukimoto, M. Saito, K. Ito, M. Murakami, and Y. Ikuhara, Phys. Rev. B **80**, 245303 (2009).
[9] M. A. Borysiewicz, E. Kamińska, A. Piotrowska, I. Pasternak, R. Jakiela, and E. Dynowska, Acta Phys. Pol. A **114**, 1061 (2008).
[10] A. Drevin-Bazin, M. F. Beaufort, M. Alkazzaz, T. Cabioch, and J. F. Barbot, Appl. Phys. Lett. **101**, 021606 (2012).
[11] J. D. Hettinger, S. E. Lofland, P. Finkel, T. Meehan, J. Palma, K. Harrell, S. Gupta, A. Ganguly, T. El-Raghy, and M. W. Barsoum, Phys. Rev. B **72**, 115120 (2005).
[12] S. E. Lofland, J. D. Hettinger, T. Meehan, A. Bryan, P. Finkel, S. Gupta, M. W. Barsoum, and G. Hug, Phys. Rev. B **74**, 174501 (2006).
[13] T. Scabarozi, A. Ganguly, J. D. Hettinger, S. E. Lofland, S. Amini, P. Finkel, T. El-Raghy, and M. W. Barsoum, J. Appl. Phys. **104**, 073713 (2008).

[14]N. Haddad, E. Garcia-Caurel, L. Hultman, M. W. Barsoum, and G. Hug, J. Appl. Phys. **104**, 023531 (2008).
[15]G. Hug, P. Eklund, and A. Orchowski, Ultramicroscopy **110**, 1054 (2010).
[16]V. Mauchamp, M. Bugnet, P. Chartier, T. Cabioc'h, M. Jaouen, J. Vinson, K. Jorissen, and J. J. Rehr, Phys. Rev. B **86**, 125109 (2012).
[17]V. Mauchamp, G. Hug, M. Bugnet, T. Cabioc'h, and M. Jaouen, Phys. Rev. B **81**, 035109 (2010).
[18]T. H. Scabarozi, P. Eklund, J. Emmerlich, H. Högberg, T. Meehan, P. Finkel, M. W. Barsoum, J. D. Hettinger, L. Hultman, and S. E. Lofland, Solid State Commun. **146**, 498 (2008).
[19]P. Eklund, M. Bugnet, V. Mauchamp, S. Dubois, C. Tromas, J. Jensen, L. Piraux, L. Gence, M. Jaouen, and T. Cabioc'h, Phys. Rev. B **84**, 075424 (2011).
[20]L. Chaput, G. Hug, P. Pécheur, and H. Scherrer, Phys. Rev. B **71**, 121104(R) (2005).
[21]M. Magnuson, M. Mattesini, N. V. Nong, P. Eklund, and L. Hultman, Phys. Rev. B **85**, 195134 (2012).
[22]L. Chaput, G. Hug, P. Pécheur, and H. Scherrer, Phys. Rev. B **75**, 035107 (2007).
[23]G. Hug, M. Jaouen, and M. W. Barsoum, Phys. Rev. B **71**, 024105 (2005).
[24]H. Högberg, L. Hultman, J. Emmerlich, T. Joelsson, P. Eklund, J. M. Molina-Aldareguia, J.-P. Palmquist, O. Wilhelmsson, and U. Jansson, Surf. Coat. Technol. **193**, 6 (2005).
[25]O. Wilhelmsson, J.-P. Palmquist, E. Lewin, J. Emmerlich, P. Eklund, P. O. A. Persson, H. Högberg, S. Li, R. Ahuja, O. Eriksson, L. Hultman, and U. Jansson, J. Cryst. Growth **291**, 290 (2006).
[26]P. Blaha, K. Schwarz, G. K. H. Madsen, D. Kvaniscka, and J. Luitz, WIEN2k, an augmented plane wave + local orbitals program for calculating crystal properties (Karlheinz Schwarz, Techn. Universität Wien, Austria, 2001), ISBN 3-9501031-1-2.
[27]E. Sjöstedt, L. Nordström, and D. J. Singh, Solid State Commun. **114**, 15 (2000).
[28]J. P. Perdew, K. Burke, and M. Ernzerhof, Phys. Rev. Lett. **77**, 3865 (1996).
[29]A. Kokalj, Comput. Mater. Sci. **28**, 155 (2003).
[30]G. K. H. Madsen and D. J. Singh, Comput. Phys. Commun. **175**, 67 (2006).
[31]M. K. Drulis, H. Drulis, S. Gupta, M. Barsoum, and T. El Raghy, J. Appl. Phys. **99**, 093502 (2006).
[32]S. E. Lofland, J. D. Hettinger, K. Harrell, P. Finkel, S. Gupta, M. Barsoum, and G. Hug, Appl. Phys. Lett. **84**, 508 (2004).
[33]L. Chaput, P. Pécheur, and H. Scherrer, Phys. Rev. B **75**, 045116 (2007).
[34]W. W. Schulz, P. B. Allen, and N. Trivedi, Phys. Rev. B **45**, 10886 (1992).
[35]M. Magnuson, O. Wilhelmsson, J.-P. Palmquist, U. Jansson, M. Mattesini, S. Li, R. Ahuja, and O. Eriksson, Phys. Rev. B **74**, 195108 (2006).
[36]G. Herranz, V. Laukhin, F. Sanchez, P. Levy, C. Ferrater, M. V. Garcìa-Cuenca, M. Varela, and J. Fontcuberta, Phys. Rev. B **77**, 165114 (2008).
[37]M. Cutler, J. F. Leavy, and R. L. Fitzpatrick, Phys. Rev. **133**, A1143 (1964).
[38]A. N. Lagarkov and A. K. Sarychev, Phys. Rev. B **53**, 6318 (1996).
[39]L. D. Landau and E. M. Lifshitz, *Electrodynamics of Continuous Media*, 2nd ed. (Pergamon, Oxford, 1984).
[40]A. Mendoza-Galvàn, M. Rybka, K. Järrendahl, H. Arwin, M. Magnuson, L. Hultman, and M. W. Barsoum, J. Appl. Phys. **109**, 013530 (2011).
[41]C. Y. Allison, F. A. Modine, and R. H. French, Phys. Rev. B **35**, 2573 (1987).